Liquid Crystals
Publication details, including instructions for authors and subscription information:
http://www.informaworld.com/smpp/title~content=t713926090

Influence of weak anchoring on flow instabilities in nematic liquid crystals

O. S. Tarasov; A. P. Krekhov; L. Kramer

Online publication date: 06 August 2010

To cite this Article Tarasov, O. S. , Krekhov, A. P. and Kramer, L.(2001) 'Influence of weak anchoring on flow instabilities in nematic liquid crystals', Liquid Crystals, 28: 6, 833 — 839

To link to this Article: DOI: 10.1080/02678290110033747

URL: http://dx.doi.org/10.1080/02678290110033747

LIQUID CRYSTALS, 2001, VOL. 28, NO. 6, 833–839

Influence of weak anchoring on flow instabilities in nematic liquid crystals

O. S. TARASOV†‡*, A. P. KREKHOV†‡ and L. KRAMER†

†Institute of Physics, University of Bayreuth, D-95440 Bayreuth, Germany

‡Institute of Molecule and Crystal Physics, Russian Academy of Sciences, 450025 Ufa, Russia

(*Received 7 August 2000; in final form 24 November 2000; accepted 1 December 2000*)

We analyse the homogeneous instabilities in a nematic liquid crystal subjected to plane steady Couette or Poiseuille flow in the case when the director is prealigned perpendicular to the flow plane taking into account weak anchoring at the confining surfaces. The critical shear rate decreases for decreasing anchoring strength and goes to zero in the limit of torque-free boundary conditions. For Poiseuille flow two types of instability arise depending on the values of the azimuthal (W_a) and polar (W_p) surface anchoring strengths. The critical line in (W_a, W_p) space which separates the two instabilities regimes is obtained.

1. Introduction

Over the last decade the study of surface anchoring in nematic liquid crystals (NLCs) for different types of confining substrates has attracted much attention. In particular, a change of anchoring strength strongly influences the orientational behaviour and dynamic response of NLCs under external electric and magnetic fields. This changes the switching times, which play an important role in applications [1]. The hydrodynamic flow is a crucial ingredient for the dynamic response and switching characteristics of liquid crystal devices.

The anchoring characteristics can also be studied in orientational phenomena induced by hydrodynamic flow. Recently in fact, the surface orientational transition caused by oscillatory shear flow was found [2] and the influence of weak anchoring on the linear response of the NLC to oscillatory flows was studied [3]. To date, the studies of orientational bulk instabilities in NLCs under hydrodynamic flow have been restricted to the case of strong surface anchoring (fixed director orientation at the confining plates) [4–6].

In this paper the influence of surface anchoring on the homogeneous instabilities in NLCs subjected to steady flow of Couette and Poiseuille types is studied theoretically for the case when the director at the bounding plates is oriented perpendicular to the flow plane. This is the simplest geometry because the initial state with the director oriented everywhere perpendicular to the flow plane is, by symmetry, a solution of the nematodynamic equations for any shear rate. The state can change only via a symmetry-breaking instability. The type of instability strongly depends on the sign of the Leslie viscosity coefficient, α_3. The case of a negative α_3 (flow-aligning materials) and strong anchoring of the director was investigated theoretically by Leslie [7] and Dubois-Violette and Manneville [5, 8–10]. They showed that in the absence of external fields the first instability is homogeneous in both steady Couette [7, 8] and Poiseuille [9] flows. The theoretical results were found to be in good agreement with the experiments of Pieranski, Guyon and coworkers [11–13]. In Couette flow, a sufficiently strong additional magnetic field applied parallel to the initial director orientation was found to change the type of instability into a spatially periodic one where rolls develop [11, 13]. This is in contrast to the case of Poiseuille flow, for which a magnetic field does not change the type of instability [14]. Well above the threshold of the homogeneous instability in Poiseuille flow, rolls were observed to develop in a secondary instability [15]. In the case of a positive α_3 (non-flow-aligning materials), according to the mechanism of Pieranski and Guyon, one has no homogeneous instability and only rolls are expected [11]. Since for these materials there is also a tumbling motion [16], the orientational behaviour of NLCs can be quite complex.

Here we focus on *flow-aligning* nematics. Starting from the standard set of nematodynamic equations in the Leslie–Ericksen formulation [4], the basic equations describing the homogeneous instabilities are presented (§2) taking into account arbitrary surface anchoring strength. Full semi-analytical solutions together with

*Author for correspondence; e-mail: oleg.tarasov@uni-bayreuth.de

Liquid Crystals ISSN 0267-8292 print/ISSN 1366-5855 online © 2001 Taylor & Francis Ltd
http://www.tandf.co.uk/journals
DOI: 10.1080/02678290110033747

approximate expressions for the critical shear rate at which the homogeneous instabilities develop are obtained for steady Couette (§ 3) and Poiseuille (§ 4) flows. In § 5 we discuss the results.

2. Basic equations

We consider a NLC layer of thickness d sandwiched between two parallel infinite plates. The origin of a Cartesian coordinate system is placed at the centre of the layer with the z axis perpendicular to the bounding plates. Steady Couette flow is generated by one plate (at $z = d/2$) moving with constant velocity V^0 along the x direction and the other plate (at $z = -d/2$) fixed. Steady Poiseuille flow is obtained when a constant pressure gradient $\Delta P/\Delta x$ is applied along the x axis. The confining plates provide a director orientation along the y axis. The basic state is given by the stationary homogeneous solution of the standard set of nematodynamic equations (Leslie–Ericksen equations [4]):

$$\mathbf{n}^0 = (0, 1, 0), \quad \mathbf{v}^0 = (v_x^0, 0, 0) \tag{1}$$

where, for Couette flow,

$$v_x^0 = V^0(1/2 + z/d) \tag{2}$$

and for Poiseuille flow,

$$v_x^0 = -\frac{\Delta P}{\Delta x}\frac{d^2}{2\eta_3}(1/4 - z^2/d^2)$$

and $\eta_3 = \alpha_4/2$ with α_4 the corresponding Leslie viscosity.

In order to investigate the stability of solution (1) we linearize the nematodynamic equations [4] with respect to perturbations that are homogeneous in the plane of the layer:

$$\mathbf{n} = \mathbf{n}^0 + (n_x, n_y, n_z), \quad \mathbf{v} = \mathbf{v}^0 + (v_x, v_y, v_z) \tag{3}$$

where n_i, v_i $(i = x, y, z)$ are functions of z. We are looking for the existence of a stationary solution of the linearized nematodynamic equations, which signals the onset of a stationary (i.e. nonoscillatory) instability. The linearized equations are:

$$\begin{aligned} \eta_1 v_{y,_{zz}} + (\eta_1 - \eta_3)(Sn_x)_{,z} &= 0 \\ \alpha_2 Sn_z - K_{22} n_{x,_{zz}} &= 0 \\ \alpha_3 Sn_x - K_{11} n_{z,_{zz}} + \alpha_3 v_{y,_z} &= 0 \end{aligned} \tag{4}$$

where $S = v^0_{x,_z}$ is the shear rate, $\eta_1 = (\alpha_3 + \alpha_4 + \alpha_6)/2$ and K_{11}, K_{22} are the elasticity coefficients for 'splay' and 'twist' deformations, respectively. The notation $f_{,z} \equiv \mathrm{d}f/\mathrm{d}z$ is used throughout.

The boundary conditions for the y-component of the velocity perturbation are

$$v_y(z = \pm d/2) = 0. \tag{5}$$

The surface anchoring of the director is described in terms of a surface energy per unit area, F_s, which has a minimum when the director at the surface is oriented along the easy axis (parallel to the y axis in our case). It is convenient to characterize the surface anchoring by a 'polar' anchoring strength W_p pertaining to out-of-substrate-plane director deviations, and an 'azimuthal' anchoring strength W_a, related to distortions within the substrate plane. A phenomenological expression for the surface energy F_s can be written in terms of an expansion with respect to $(\mathbf{n} - \mathbf{n}^0)$. For small director deviations from the easy axis, one obtains for the surface energy

$$F_s = \frac{1}{2}W_a n_x^2 + \frac{1}{2}W_p n_z^2, \quad W_a > 0, W_p > 0. \tag{6}$$

The boundary conditions for the director perturbations can be obtained from the surface torques balance equation

$$\pm K_{22} n_{x,_z} + \frac{\partial F_s}{\partial n_x} = 0, \quad \pm K_{11} n_{z,_z} + \frac{\partial F_s}{\partial n_z} = 0,$$
$$\text{for } z = \pm d/2. \tag{7}$$

Introducing the dimensionless quantities

$$\begin{aligned} \tilde{z} &= \frac{z}{d}, \quad \tilde{S} = \beta\tau_d S, \quad \tau_d = \frac{(-\alpha_2)d^2}{K_{22}} \\ V_y &= \frac{\beta^2 b\tau_d}{d} v_y, \quad N_x = \beta n_x, \quad N_z = n_z \end{aligned} \tag{8}$$

with

$$\beta^2 = \frac{\alpha_3}{\alpha_2}\frac{K_{22}}{K_{11}}\frac{1}{b}, \quad b = \frac{\eta_1}{\eta_3}, \tag{9}$$

equations (4) can be rewritten in the form

$$\begin{aligned} V_{y,_{zz}} - (1 - b)(\tilde{S}N_x)_{,z} &= 0 \\ \tilde{S}N_z + N_{x,_{zz}} &= 0 \\ b\tilde{S}N_x + N_{z,_{zz}} + V_{y,_z} &= 0. \end{aligned} \tag{10}$$

For the shear rate $\tilde{S}$ one has, for Couette flow,

$$\tilde{S} = a^2, \quad a^2 = \frac{V^0\tau_d}{d}\beta \tag{11}$$

and for Poiseuille flow,

$$\tilde{S} = -a^2 z, \quad a^2 = -\frac{\Delta P}{\Delta x}\frac{\tau_d d}{\eta_3}\beta. \tag{12}$$

The boundary conditions (5) and (7) reduced to

$$\begin{aligned} &\pm N_{x,_z} + w_a N_x = 0, \quad \pm N_{z,_z} + w_p N_z = 0, \\ &V_y = 0, \quad \text{at } z = \pm 1/2 \end{aligned} \tag{13}$$

where

$$w_a = W_a d/K_{22}, \quad w_p = W_p d/K_{11}. \qquad (14)$$

In the limit of strong anchoring ($w_a, w_p \to \infty$) one has $N_x = N_z = 0$ at $z = \pm 1/2$ whereas for torque-free boundary conditions ($w_a, w_p \to 0$) $N_{x,_z} = N_{z,_z} = 0$ at the boundaries. From equations (14) one can see that by changing the thickness d, the dimensionless anchoring strengths w_a and w_p can be varied, the ratio w_a/w_p remaining fixed.

Solving the system of linear ordinary differential equations (10) with boundary conditions (13) one can obtain the critical value of the shear rate a_c^2, at which the initial state (1) loses stability, and determine the influence of anchoring strengths w_a and w_p on a_c^2.

3. Couette flow

In this case the shear rate $\tilde{S}$ is independent of z (11), so that the system (10) can be solved using the standard theory of ordinary differential equations with constant coefficients. Further, the $\{z \to -z\}$ symmetry of equations (10) allows for two possible types of solutions:

I: $\{V_y$-even; N_x, N_z-odd$\}$-'odd' solution

II: $\{V_y$-odd; N_x, N_z-even$\}$-'even' solution.

We will always classify the solutions by the z-symmetry of the x-component of the director perturbation N_x. For the *odd* solution one obtains

$$\begin{aligned} V_y &= C_1(1-b)a\cosh(az) - C_2(1-b)a\cos(az) + C_3 \\ N_x &= C_1\sinh(az) + C_2\sin(az) \\ N_z &= -C_1\sinh(az) + C_2\sin(az). \end{aligned} \qquad (15)$$

Taking into account the boundary conditions (13) the solvability condition for the C_i ('boundary determinant' equated to zero) gives the expression for the critical shear rate

$$\begin{aligned} &2w_a w_p \sinh(a_c/2)\sin(a_c/2) + a_c(w_a + w_p) \\ &\times[\cosh(a_c/2)\sin(a_c/2) + \cos(a_c/2)\sinh(a_c/2)] \\ &+ 2a_c^2\cosh(a_c/2)\cos(a_c/2) = 0. \end{aligned} \qquad (16)$$

For the *even* solution one obtains

$$\begin{aligned} V_y &= C_1(1-b)a\sinh(az) + C_2(1-b)a\sin(az) - C_3 a^2 bz \\ N_x &= C_1\cosh(az) + C_2\cos(az) + C_3 \\ N_z &= -C_1\cosh(az) + C_2\cos(az). \end{aligned} \qquad (17)$$

The boundary determinant condition now gives

$$\begin{aligned} &a_c^3 b\sinh(a_c/2)\sin(a_c/2) + \frac{1}{2}a_c^2 b(w_a + w_p) \\ &\times[\cosh(a_c/2)\sin(a_c/2) - \cos(a_c/2)\sinh(a_c/2)] \\ &-\{a_c b\cosh(a_c/2)\cos(a_c/2) \\ &+(1-b)[\sinh(a_c/2)\cos(a_c/2) \\ &+\sin(a_c/2)\cosh(a_c/2)]\}w_a w_p = 0. \end{aligned} \qquad (18)$$

It should be noted, that the expressions (16) and (18) are both symmetric under exchange of w_a and w_p. This results from the fact that N_x and N_z have the same symmetry. We found that for MBBA material parameters at 25°C [17] ($b = 0.58$) the critical shear rate for the *odd* mode is systematically higher than for the *even* mode, so there is no transition between them under a variation of the surface anchoring. For strong anchoring ($w_a = w_p = \infty$) the expression for the critical shear rate of the *even* solution (18) recovers the result obtained by Leslie [7]. Weak surface anchoring reduces the critical shear rate compared with the case of strong boundary conditions. In the limit of one of the surface anchoring strengths going to zero ($w_a \to 0$ or $w_p \to 0$) one has $a_c^2 \to 0$. In figure 1 the critical shear rate a_c^2 for the *even* solution calculated from equation (18), using the material parameters of MBBA ($b = 0.58$), is shown as a function of $1/w_a$, $1/w_p$.

In order to obtain an easy-to-use expression for the critical shear rate of the relevant *even* mode as a function of the surface anchoring strengths, one can use the single-mode approximation in the spirit of a Galerkin expansion [18]. We choose

$$\begin{aligned} V_y &= C_1\sin(2\pi z) \\ N_x &= C_2[w_a\cos(\pi z) + \pi] \\ N_z &= C_3[w_p\cos(\pi z) + \pi] \end{aligned} \qquad (19)$$

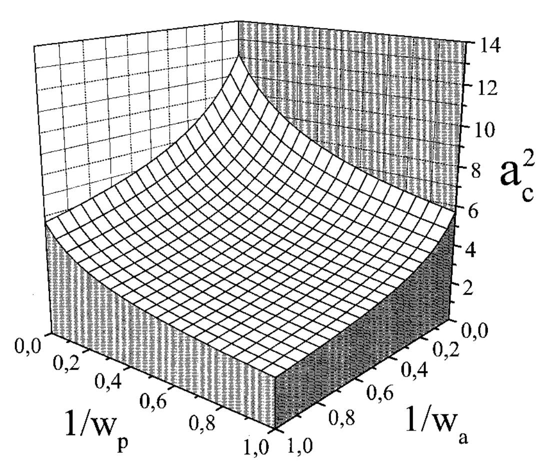

Figure 1. Critical shear rate of Couette flow vs. anchoring strengths: $b = 0.58$ (MBBA).

which satisfy boundary conditions (13). Substituting this ansatz into equations (10) where $\tilde{S} = a^2$ and solving the algebraic system for C_i, $(i = 1, 2, 3)$ obtained after projecting the first of equations (10) onto the first mode of equations (19), the second equation onto the second mode, etc., one gets

$$\begin{aligned} a_c^2 &= 3\pi^3 [w_a w_p (4 + w_a)(4 + w_p)/(p_1 p_2)]^{1/2} \\ p_1 &= w_a w_p + 4(w_a + w_p) + 2\pi^2 \\ p_2 &= 16 w_a w_p (1 - b) + 9\pi^2 b p_1. \end{aligned} \tag{20}$$

The single-mode approximation (20) gives almost the same values for a_c^2 as equation (18) (the relative error is smaller than 1%), so that they could not be differentiated in figure 1.

4. Poiseuille flow

In the case of Poiseuille flow, the shear rate $\tilde{S}$ is given by equation (12) and the symmetry properties of system (10) give us the following two types of solutions:

I: $\{V_y, N_x\text{-odd}; N_z\text{-even}\}$-'odd' solution

II: $\{V_y, N_x\text{-even}; N_z\text{-odd}\}$-'even' solution.

The *odd* solution corresponds to the *splay*-mode and the *even* solution to the *twist*-mode in the notation of Dubois-Violette and Manneville [9]. Integration of the first equation in system (10) gives

$$V_{y,_z} = K - (1 - b) a^2 z N_x \tag{21}$$

with $K = 0$ for the *even* solution. For the *odd* solution the integration constant K must be non-zero (except for $b = 1$, see later). After eliminating $V_{y,_z}$ from the third equation in (10) one arrives at

$$\begin{aligned} a^2 z N_z - N_{x,_{zz}} &= 0 \\ a^2 z N_x - N_{z,_{zz}} &= K. \end{aligned} \tag{22}$$

Following [9] we perform the transformation $Z = a^{2/3} z$ and introduce new variables $\mathcal{U} = N_x + N_z$, $\mathcal{V} = N_x - N_z$, leading to

$$\begin{aligned} \mathcal{U}_{,ZZ} - Z\mathcal{U} &= -K a^{-4/3} \\ \mathcal{V}_{,ZZ} + Z\mathcal{V} &= K a^{-4/3}. \end{aligned} \tag{23}$$

The general solution of (23) can be expressed in terms of Airy functions $Ai(Z)$, $Bi(Z)$, $Gi(Z)$ [19].

Let us first consider the case of the *even* solution $(K = 0)$, then one has

$$\begin{aligned} N_x &= C_1[Ai(Z) + Ai(-Z)] + C_2[Bi(Z) + Bi(-Z)] \\ N_z &= C_1[Ai(Z) - Ai(-Z)] + C_2[Bi(Z) - Bi(-Z)] \end{aligned} \tag{24}$$

where C_1 and C_2 are constants to be determined from the boundary conditions (13). Substitution of equations (24) into (13) gives the criterion for the threshold shear rate,

$$\frac{w_a Ai^+ + a_c^{2/3} Ai^+_{,Z}}{w_a Bi^+ + a_c^{2/3} Bi^+_{,Z}} = \frac{w_p Ai^- + a_c^{2/3} Ai^-_{,Z}}{w_p Bi^- + a_c^{2/3} Bi^-_{,Z}}. \tag{25}$$

Here

$$\begin{aligned} Ai^\pm &= Ai\left(\frac{1}{2} a_c^{2/3}\right) \pm Ai\left(-\frac{1}{2} a_c^{2/3}\right), \\ Bi^\pm &= Bi\left(\frac{1}{2} a_c^{2/3}\right) \pm Bi\left(-\frac{1}{2} a_c^{2/3}\right) \end{aligned} \tag{26}$$

and similarly for $Ai^\pm_{,Z}$ and $Bi^\pm_{,Z}$. The limit of strong anchoring $(w_a \to \infty, w_p \to \infty)$ gives the result of Dubois-Violette and Manneville [9]

$$\frac{Ai\left(\frac{1}{2} a_c^{2/3}\right)}{Bi\left(\frac{1}{2} a_c^{2/3}\right)} = \frac{Ai\left(-\frac{1}{2} a_c^{2/3}\right)}{Bi\left(-\frac{1}{2} a_c^{2/3}\right)}$$

leading to $a_c^2 = 102.59$. The fact that N_x and N_z have different z-symmetry leads in equation (25) to an asymmetry in the dependence of the critical shear rate on w_a and w_p, in contrast to the case of Couette flow. The critical shear rate, equation (25), retains a finite value when the polar anchoring strength w_p (which mainly controls N_z perturbations) vanishes, whereas $a_c^2 \to 0$ if the azimuthal anchoring strength $w_a \to 0$.

For the *odd* solution with a non-zero K the solution of equations (22) has the following form

$$\begin{aligned} N_x &= kK\{C_1 Ai^-(Z) + C_2 Bi^-(Z) + Gi^-(Z)\} \\ N_z &= kK\{C_1 Ai^+(Z) + C_2 Bi^+(Z) + Gi^+(Z)\} \end{aligned} \tag{27}$$

where

$$k = \pi a^{-4/3}/2, \quad Ai^\pm(Z) = Ai(Z) \pm Ai(-Z) \text{ etc., for } Bi^\pm(Z) \text{ and } Gi^\pm(Z). \tag{28}$$

The coefficients C_i in equations (27) are determined from the boundary conditions (13). Integrating equation (21) and taking into account the boundary conditions $V_y(z = \pm 1/2) = 0$, one obtains the expression for the critical shear rate of the *odd* mode,

$$K - (1 - b) a_c^2 \int_{-1/2}^{1/2} z N_x(z; a_c^2, w_a, w_p)\, dz = 0. \tag{29}$$

Since N_x is proportional to K, this undetermined integration constant falls out from equation (29). From thermodynamical conditions [4, 20] the parameter b must be positive, but is otherwise not restricted. The point $b = 1$ requires special consideration. In this case, from equation (21) and boundary conditions for V_y, it follows that $K = 0$ and $V_y = 0$, so that one should solve equations (22) keeping the symmetry of N_x and N_z corresponding to the *odd* solution. In other words, if $b = 1$ then one has the homogeneous instability of *odd* type with zero velocity perturbation, as in the case of a Fréedericksz transition. Moreover, in the case $b = 1$ equations (22) became invariant with respect to change $\{N_x \Leftrightarrow N_z\}$, so that the critical shear rates for *even* and *odd* solutions are the same up to transposition $\{w_a \Leftrightarrow w_p\}$.

The instability of the *odd* mode is mainly controlled by the polar anchoring strength w_p. In the limit of zero azimuthal anchoring strength, $w_a \to 0$, one has a finite critical shear rate, whereas $a_c^2 \to 0$ for the polar anchoring strength $w_p \to 0$.

The critical shear rate a_c^2 for the *even* solution, equation (25), and *odd* solution, equation (29), have been calculated for the material parameters of MBBA for various values of w_a and w_p (figure 2). Depending on the azimuthal and polar surface anchoring strengths, one can have a different z-symmetry of the first unstable mode. The critical line in (w_a, w_p) space corresponds to the crossover between the two types of unstable solutions.

Since the expressions (25) and (29) for the critical shear rates of the two possible unstable modes are quite complicated we use a single-mode Galerkin approximation in order to obtain easy-to-use formulae.

For the *even* mode we can use equations (22) with $K = 0$. Assuming,

$$\begin{aligned} N_x &= C_1[w_a \cos(\pi z) + \pi] \\ N_z &= C_2[w_p \sin(2\pi z) + 2\pi \sin(\pi z)] \end{aligned} \tag{30}$$

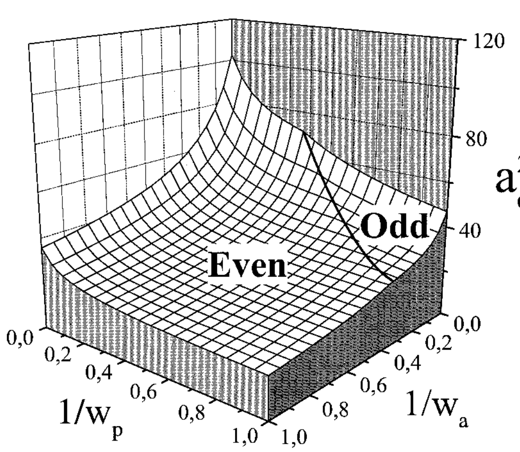

Figure 2. Critical shear rate of Poiseuille flow vs. anchoring strengths: $b = 0.58$ (MBBA).

and after substituting (30) into (22) and projection, one obtains

$$\begin{aligned} a_c^2 &= 6\sqrt{3}\pi^4[w_a(4 + w_a)(3\pi^2 + 20w_p + 3w_p^2)/p_1^2]^{1/2} \\ p_1 &= 16w_a w_p + 9\pi^2(w_a + w_p) + 72\pi^2. \end{aligned} \tag{31}$$

For the *odd* mode we choose

$$\begin{aligned} N_x &= C_1[w_a \sin(2\pi z) + 2\pi \sin(\pi z)] \\ N_z &= C_2[w_p \cos(\pi z) + \pi]. \end{aligned} \tag{32}$$

Substituting these into (22) one finds the coefficients C_1 and C_2 and then from (29) one obtains,

$$\begin{aligned} a_c^2 &= 6\sqrt{3}\pi^4[w_p(4 + w_p)(3\pi^2 + 20w_a + 3w_a^2)/(p_1 p_2)]^{1/2} \\ p_2 &= bp_1 + (1 - b)(9\pi^2 - 144 - 2w_a)w_p. \end{aligned} \tag{33}$$

The approximate expressions (31) and (33) give systematically higher values for the critical shear rate compared with (25) and (29), specifically, about 10% for both modes. Equating (31) and (33) one can obtain an approximate expression for the critical line in the (w_a, w_p) plane corresponding to the crossover between the critical *even* and *odd* modes (see figure 2). We now write $\beta_a = 1/w_a$, $\beta_p = 1/w_p$. For strong azimuthal anchoring $(\beta_a = 0)$ the transition from *even* to *odd* mode takes place at some critical value of polar anchoring strength; $\beta_p = \beta_{p0}$, where β_{p0} is the solution of the algebraic equation

$$9\pi^4 b\beta_{p0}^3 + 2\pi^2(39b - 19)\beta_{p0}^2 + \left[-9\pi^2(1 - b) + 120b - \frac{232}{3}\right]\beta_{p0} - 18(1 - b) = 0. \tag{34}$$

For MBBA material parameters one finds $\beta_{p0} = 0.307$. Assuming the deviation $(\hat{\beta}_a, \hat{\beta}_p)$ from $(0, \beta_{p0})$ to be small, one has up to first order in $\hat{\beta}_a, \hat{\beta}_p$ for the critical line

$$c_1(\beta_{p0} + \hat{\beta}_p) + c_2\hat{\beta}_a = 0 \tag{35}$$

where

$$\begin{aligned} c_1 &= 27b\pi^4\beta_{p0}^2 + 4\pi^2(39b - 19)\beta_{p0} \\ &\quad - 9\pi^2(1 - b) + 120b - \frac{232}{3} \\ c_2 &= 108b\pi^4\beta_{p0}^3 + \pi^2(9b\pi^2 + 936b - 680)\beta_{p0}^2 \\ &\quad - 36(3\pi^2 + 40)(1 - b)\beta_{p0} + 216b - \frac{776}{3}. \end{aligned} \tag{36}$$

The results for the critical line for the crossover between *even* and *odd* critical modes obtained from the numerical solutions of equations (25) and (29) and the approximation (35) are shown in figure 3.

Note, that $\beta_a = 1/w_a$ and $\beta_p = 1/w_p$ are inversely proportional to the thickness d of the NLC layer. Therefore, by varying the cell thickness, one can cross the critical line separating the two regimes. For that purpose it is necessary to have the ratio $\beta_p/\beta_a \equiv K_{11}W_a/(K_{22}W_p)$ larger than the slope of the critical line ($\sim -c_2/c_1$). Using the material parameters of MBBA one obtains $W_a/W_p > -c_2K_{22}/(c_1K_{11}) = 2.28$ ($W_a/W_p > 1.78$ from numerical results). For small values of w_a and w_p, the crossover is given by $w_a = w_p/b$. As was said above, if $b = 1$, equations (22) are invariant with respect to $\{N_x \Leftrightarrow N_z\}$. This means that the crossover line for $b = 1$ is exactly defined by $w_a = w_p$. The same result follows from the approximate formulae (31) and (33).

5. Conclusions and discussion

It was found that changes of the anchoring strengths can cause a crossover between two types of homogeneous instability induced by steady Poiseuille flow, in contrast to the case of steady Couette flow, where the first unstable mode is always the *even* one. Semi-analytical expressions for the critical shear rates for both Poiseuille and Couette flow are presented, together with simple approximate formulae of good accuracy.

The effect of the reduction of the critical shear rate for homogeneous instabilities under weak surface anchoring can, in principle, be used for the determination of the polar (W_p) and azimuthal (W_a) anchoring strengths. For that purpose one may measure the critical shear rates for two cells with different thicknesses and use the full expressions (or approximate formulae) to calculate both W_p and W_a. Alternatively, one can use an additional electric field applied across the NLC cell. Depending on the sign of the dielectric anisotropy of the NLC, the electric field will stabilize or destabilize n_z fluctuations and affect the critical shear rate differently for different values of the polar and azimuthal anchoring strengths. This study is in progress. The advantage of using measurements of the critical shear rate for the determination of polar and azimuthal anchoring strengths, compared with the other methods (Fréedericksz transition, orientational transition with hybrid orientation, small angle light scattering), is that here one does not need to modify (or rebuild) the experimental set-up in order to obtain W_p and W_a at the same time.

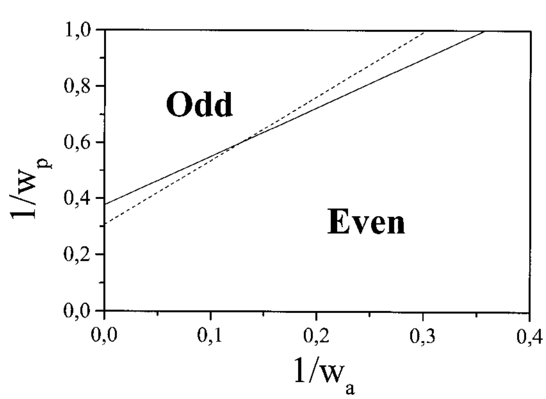

Figure 3. Critical line separating *odd* and *even* regimes in Poiseuille flow: numerical solution (solid) and approximation (35) (dotted), $b = 0.58$ (MBBA).

It would be particularly interesting to investigate experimentally the orientational behaviour of NLC under steady Poiseuille flow for a cell with W_p, W_a close to the crossover line separating critical modes of different symmetry.

Financial support of Deutscher Akademischer Austauschdienst (DAAD), DFG (Grant Kr690/14-1) and INTAS (Grant 96-498) are gratefully acknowledged. O.T. and A.K. wish to thank the University of Bayreuth for its hospitality.

References

[1] See, for example: Chigrinov, V. G., 1999, *Liquid Crystals Devices: Physics and Applications* (New York: Artech House).

[2] Khazimullin, M. V., Börzsönyi, T., Krekhov, A. P., and Lebedev, Yu. A., 1999, *Mol. Cryst. liq. Cryst.*, **329,** 247.

[3] Nasibullayev, I. Sh., Krekhov, A. P., and Khazimullin, M. V., 2000, *Mol. Cryst. liq. Cryst.*, **351,** 395.

[4] Leslie, F. M., 1979, *Adv. liq. Cryst.*, **4,** 1.

[5] Dubois-Violette, E., and Manneville, P., 1996, in *Pattern Formation in Liquid Crystals*, edited by A. Buka and L. Kramer (Berlin: Springer-Verlag), pp. 91–164.

[6] Krekhov, A. P., Börzsönyi, T., Tòth, P., Buka, À., and Kramer, L., 2000, *Phys. Rep.*, **337,** 171.

[7] Leslie, F. M., 1976, *J. Phys. D: appl. Phys.*, **9,** 925.

[8] Manneville, P., and Dubois-Violette, E., 1976, *J. Phys. (Fr.)*, **37,** 285.

[9] Manneville, P., and Dubois-Violette, E., 1976, *J. Phys. (Fr.)*, **37,** 1115.

[10] Manneville, P., 1979, *J. Phys. (Fr.)*, **40,** 713.

[11] Pieranski, P., and Guyon, E., 1974, *Phys. Rev. A*, **9,** 404.

[12] Pieranski, P., and Guyon, E., 1973, *Solid State Commun.*, **13,** 435; Pieranski, P., and Guyon, E., 1976, *Commun. Phys.*, **1,** 45.

[13] Dubois-Violette, E., Guyon, E., Janossy, I., Pieranski, P., and Manneville, P., 1977, *J. Mec.*, **16,** 734.

[14] Janossy, I., Pieranski, P., and Guyon, E., 1976, *J. Phys. (Fr.)*, **37,** 1105.

[15] Guyon, E., and Pieranski, P., 1975, *J. Phys. (Fr.)*, **36,** C1-203.

[16] Pikin, S. A., 1974, *Sov. Phys. JETP*, **38,** 1246; Pieranski, P., Guyon, E., and Pikin, S. A., 1976, *J. Phys. Colloq. Paris*, **37,** C1-3; Cladis, P. E., and Torza, S., 1975, *Phys. Rev. Lett.*, **35,** 1283.

[17] Kneppe, H., Schneider, F., and Sharma, N. K., 1982, *J. chem. Phys.*, **77,** 3203; de Jeu, W. H., Claassen, W. A. P., and Spruijt, A. M. J., 1976, *Mol. Cryst. liq. Cryst.*, **37,** 269.

[18] Gottlieb, D., and Orszag, S. A., 1993, *Numerical Analysis of Spectral Methods: Theory and Applications* (Montpelier: Capital City Press); Pesch, W., and Kramer, L., 1996, in *Pattern Formation in Liquid Crystals*, edited by A. Buka and L. Kramer (Berlin: Springer-Verlag), pp. 69–90.

[19] See, for example; Abramowitz, M., and Stegun, I. A., 1964, *Handbook of Mathematical Functions* (New York: Dover) Chap. 10.

[20] Pleiner, H., and Brand, H. R., 1996, in *Pattern Formation in Liquid Crystals*, edited by A. Buka and L. Kramer (Berlin: Springer-Verlag), pp. 15–68.